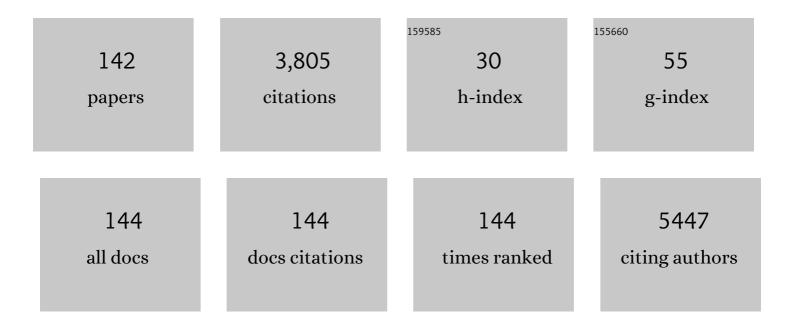
Cinzia Cepek

List of Publications by Year in descending order

Source: https://exaly.com/author-pdf/6795732/publications.pdf Version: 2024-02-01



#	Article	IF	CITATIONS
1	In situ Observations of Catalyst Dynamics during Surface-Bound Carbon Nanotube Nucleation. Nano Letters, 2007, 7, 602-608.	9.1	662
2	In-situ X-ray Photoelectron Spectroscopy Study of Catalystâ^'Support Interactions and Growth of Carbon Nanotube Forests. Journal of Physical Chemistry C, 2008, 112, 12207-12213.	3.1	240
3	<i>In Situ</i> Observations of the Atomistic Mechanisms of Ni Catalyzed Low Temperature Graphene Growth. ACS Nano, 2013, 7, 7901-7912.	14.6	163
4	Nanostructured TiO2 Films with 2 eV Optical Gap. Advanced Materials, 2005, 17, 1842-1846.	21.0	148
5	Chemisorption and fragmentation of C60 Pt(111) and Ni(110). Physical Review B, 1996, 53, 7466-7472.	3.2	124
6	Stable, efficient p-type doping of graphene by nitric acid. RSC Advances, 2016, 6, 113185-113192.	3.6	66
7	Binding and ordering of C60 on Pd(110): Investigations at the local and mesoscopic scale. Journal of Chemical Physics, 2001, 115, 9001-9009.	3.0	63
8	Supportâ^'Catalystâ^'Gas Interactions during Carbon Nanotube Growth on Metallic Ta Films. Journal of Physical Chemistry C, 2011, 115, 4359-4369.	3.1	60
9	1.5 MeV proton irradiation effects on electrical and structural properties of TiO2/n-Si interface. Journal of Applied Physics, 2014, 115, .	2.5	58
10	Photoemission study ofC60/Si(111)adsorption as a function of coverage and annealing temperature. Physical Review B, 1999, 60, 2068-2073.	3.2	57
11	Step-by-Step Growth of HKUST-1 on Functionalized TiO2 Surface: An Efficient Material for CO2 Capture and Solar Photoreduction. Catalysts, 2018, 8, 353.	3.5	52
12	Low temperature growth of ultra-high mass density carbon nanotube forests on conductive supports. Applied Physics Letters, 2013, 103, .	3.3	49
13	Stability of graphene doping with MoO3 and I2. Applied Physics Letters, 2014, 105, .	3.3	49
14	Electronic structure and molecular orientation of a Zn-tetra-phenyl porphyrin multilayer on Si(111). Surface Science, 2006, 600, 4013-4017.	1.9	44
15	Heterogeneous and Homogeneous Routes in Water Oxidation Catalysis Starting from Cu ^{II} Complexes with Tetraaza Macrocyclic Ligands. Chemistry - an Asian Journal, 2016, 11, 1281-1287.	3.3	43
16	Cerium conversion coating and sol–gel multilayer system for corrosion protection of AA6060. Surface and Coatings Technology, 2016, 287, 33-43.	4.8	43
17	Temperature-Dependent Fermi Gap Opening in thec(6×4)–C60/Ag(100)Two-Dimensional Superstructure. Physical Review Letters, 2001, 86, 3100-3103.	7.8	41
18	Mesoscopic Donorâ^'Acceptor Multilayer by Ultrahigh-Vacuum Codeposition of Zn-Tetraphenyl-Porphyrin and C70. Journal of the American Chemical Society, 2009, 131, 644-652.	13.7	41

#	Article	IF	CITATIONS
19	First-order orientational-disordering transition on the (111) surface ofC60. Physical Review B, 1996, 54, 2890-2895.	3.2	39
20	Efficient Transfer Doping of Carbon Nanotube Forests by MoO ₃ . ACS Nano, 2015, 9, 10422-10430.	14.6	39
21	Effect of substrate surface defects on the morphology of Fe film deposited on graphite. Surface Science, 2007, 601, 188-192.	1.9	38
22	Experimental and Theoretical Investigation on the Catalytic Generation of Environmentally Persistent Free Radicals from Benzene. Journal of Physical Chemistry C, 2017, 121, 9381-9393.	3.1	38
23	Brillouin-scattering determination of the elastic constants of epitaxial fccC60film. Physical Review B, 1995, 52, R8707-R8710.	3.2	37
24	Use of plasma treatment to grow carbon nanotube forests on TiN substrate. Journal of Applied Physics, 2011, 109, .	2.5	37
25	Coexisting inequivalent orientations of C60 on Ag(001). Physical Review B, 2001, 63, .	3.2	35
26	Drug Salt Formation via Mechanochemistry: The Case Study of Vincamine. Molecular Pharmaceutics, 2013, 10, 211-224.	4.6	35
27	Stability of benzotriazole-based films against AA2024 aluminium alloy corrosion process in neutral chloride electrolyte. Journal of Alloys and Compounds, 2018, 735, 2512-2522.	5.5	34
28	Enhanced Oral Bioavailability of Vinpocetine Through Mechanochemical Salt Formation: Physico-Chemical Characterization and In Vivo Studies. Pharmaceutical Research, 2011, 28, 1870-1883.	3.5	33
29	Temperature and momentum dependence of the spectral function of the charge-density wave and of the normal α phase of Pb/Ge(111). Physical Review B, 1997, 55, 4109-4112.	3.2	32
30	Structural reorganization of carbon nanoparticles into single-wall nanotubes. Physical Review B, 2002, 66, .	3.2	32
31	Switchable graphene-substrate coupling through formation/dissolution of an intercalated Ni-carbide layer. Scientific Reports, 2016, 6, 19734.	3.3	31
32	Low temperature growth of carbon nanotubes on tetrahedral amorphous carbon using Fe–Cu catalyst. Carbon, 2015, 81, 639-649.	10.3	30
33	Temperature dependence of the electronic structure nearEFand electron-phonon interaction inC60/Ag(100)single layers. Physical Review B, 1998, 58, 2228-2232.	3.2	29
34	Electronic structure of K doped C60 monolayers on Ag(001). Surface Science, 2000, 454-456, 467-471.	1.9	28
35	Substrate-adlayer interaction at the interface studied by high-resolution synchrotron radiation. Surface Science, 1997, 377-379, 1066-1070.	1.9	27
36	Temperature-Driven Changes of the Graphene Edge Structure on Ni(111): Substrate vs Hydrogen Passivation. Nano Letters, 2015, 15, 56-62.	9.1	27

#	Article	IF	CITATIONS
37	Controlled growth of zinc oxide nanorods synthesised by the hydrothermal method. Thin Solid Films, 2015, 578, 7-10.	1.8	27
38	Low-Temperature Growth of Carbon Nanotube Forests Consisting of Tubes with Narrow Inner Spacing Using Co/Al/Mo Catalyst on Conductive Supports. ACS Applied Materials & Interfaces, 2015, 7, 16819-16827.	8.0	27
39	Free surfaces recast superconductivity in few-monolayer MgB2: Combined first-principles and ARPES demonstration. Scientific Reports, 2017, 7, 14458.	3.3	27
40	Graphene on nickel (100) micrograins: Modulating the interface interaction by extended moiré superstructures. Carbon, 2018, 130, 441-447.	10.3	27
41	Molecular orientations, electronic properties and charge transfer timescale in a Zn-porphyrin/C70 donor–acceptor complex for solar cells. Surface Science, 2006, 600, 4018-4023.	1.9	26
42	Ferromagnetic and ordered MnSi(111) epitaxial layers. Applied Physics Letters, 2010, 96, .	3.3	26
43	One-dimensional chains of C60 molecules on Cu(221). Surface Science, 2004, 566-568, 633-637. (2 <mml:math)="" 0="" 10="" 482<="" 50="" etqq0="" overlock="" rgbt="" td="" tf="" tj="" xmlns:mml="http://www.w3.org/1998/Math/MathML"><td>1.9 Td (display</td><td>25 /="inline"> <m< td=""></m<></td></mml:math>	1.9 Td (display	25 /="inline"> <m< td=""></m<>
44	xmlns:mml="http://www.w3.org/1998/Math/MathML" display="inline"> <mml:mrow><mml:mi>R</mml:mi><mml:msup><mml:mn>30</mml:mn><mml:mo>â^~self-assembly ordering by C<mml:math <="" td="" xmlns:mml="http://www.w3.org/1998/Math/MathML"><td>າo>³;7mml:</td><td>:msup></td></mml:math></mml:mo></mml:msup></mml:mrow>	າo> ³ ;7mml:	:msup>
45	display="inline", < mml. Physical Review B, 2012, 86 Insight into the Influence of ZnO Defectivity on the Catalytic Generation of Environmentally Persistent Free Radicals in ZnO/SiO ₂ Systems. Journal of Physical Chemistry C, 2019, 123, 21651-21661.	3.1	25
46	Epitaxial growth of MgB2(0001) thin films on magnesium single-crystals. Applied Physics Letters, 2004, 85, 976-978.	3.3	24
47	Interface formation and growth of ferromagnetic thin layers in the Mn:Ge(111) system probed by dichroic soft x-ray spectroscopies. Physical Review B, 2007, 75, .	3.2	24
48	Growth of curved graphene sheets on graphite by chemical vapor deposition. Physical Review B, 2009, 79, .	3.2	24
49	Substrate Influence for the Znâ€ŧetraphenylâ€porphyrin Adsorption Geometry and the Interfaceâ€induced Electron Transfer. ChemPhysChem, 2010, 11, 2248-2255.	2.1	24
50	Electrical conduction of carbon nanotube forests through sub-nanometric films of alumina. Applied Physics Letters, 2013, 102, .	3.3	24
51	The surface triplet exciton of C60(111). Synthetic Metals, 1996, 77, 189-194.	3.9	23
52	Catalytic chemical vapor deposition of methane on graphite to produce graphene structures. Carbon, 2010, 48, 1619-1625.	10.3	23
53	Chiral Conformation at a Molecular Level of a Propeller-Like Open-Shell Molecule on Au(111). Journal of Physical Chemistry Letters, 2012, 3, 1559-1564.	4.6	22
54	Controlled synthesis of carbon nanostructures using aligned ZnO nanorods as templates. Carbon, 2012, 50, 5472-5480.	10.3	22

#	Article	IF	CITATIONS
55	Rationale of using Vinca minor Linne dry extract phytocomplex as a vincamine's oral bioavailability enhancer. European Journal of Pharmaceutics and Biopharmaceutics, 2013, 84, 138-144.	4.3	22
56	Surface phase transitions of Ge(100) from temperature-dependent valence-band photoemission. Physical Review B, 1998, 57, 14654-14657.	3.2	21
57	Element-Specific Probe of the Magnetic and Electronic Properties of Dyincar-Fullerenes. Journal of Physical Chemistry B, 2006, 110, 7289-7295.	2.6	21
58	Interplay among work function, electronic structure and stoichiometry in nanostructured VOx films. Physical Chemistry Chemical Physics, 2020, 22, 6282-6290.	2.8	21
59	"Inside out―growth method for high-quality nitrogen-doped graphene. Carbon, 2021, 171, 704-710.	10.3	20
60	The EEL epectrum of the triplet exciton of C60 and the theoretical analysis of its vibronic structure. Chemical Physics Letters, 1996, 250, 537-543.	2.6	19
61	Electron transfer fromGdions to theCcage in endohedralGd@C82probed by resonant photoemission spectroscopy. Physical Review B, 2004, 70, .	3.2	17
62	Optical and electrical characteristics of 17 keV X-rays exposed TiO 2 films and Ag/TiO 2 / p -Si MOS device. Materials Science in Semiconductor Processing, 2017, 63, 107-114.	4.0	17
63	Operando atomic-scale study of graphene CVD growth at steps of polycrystalline nickel. Carbon, 2020, 161, 528-534.	10.3	17
64	Electronic structure and growth mode of the early stages of C60 adsorption at the Ag(001) surface. Surface Science, 2000, 454-456, 766-770.	1.9	16
65	C70 adsorbed on Cu(111): Metallic character and molecular orientation. Journal of Chemical Physics, 2002, 116, 7685-7690.	3.0	16
66	Core Level Photoemission Evidence of Frustrated Surface Molecules: A Germ of Disorder at the (111) Surface ofC60before the Order-Disorder Surface Phase Transition. Physical Review Letters, 2002, 88, 196102.	7.8	16
67	Surface-bound chemical vapour deposition of carbon nanotubes: In situ study of catalyst activation. Physica E: Low-Dimensional Systems and Nanostructures, 2008, 40, 2238-2242.	2.7	16
68	High resolution photoemission study of C60 on Si(111) as a precursor of SiC growth. Surface Science, 2000, 454-456, 832-836.	1.9	15
69	Growth of multi-wall and single-wall carbon nanotubes with in situ high vacuum catalyst deposition. Carbon, 2004, 42, 440-443.	10.3	15
70	Tantalum-oxide catalysed chemical vapour deposition of single- and multi-walled carbon nanotubes. RSC Advances, 2013, 3, 4086.	3.6	15
71	Gd-Enhanced Growth of Multi-Millimeter-Tall Forests of Single-Wall Carbon Nanotubes. ACS Nano, 2019, 13, 13208-13216.	14.6	15
72	Characterization of high-quality MgB2(0001) epitaxial films on Mg(0001). New Journal of Physics, 2006, 8. 12-12.	2.9	14

#	Article	IF	CITATIONS
73	Carbon nanotube growth on conductors: Influence of the support structure and catalyst thickness. Carbon, 2014, 73, 13-24.	10.3	14
74	The synergistic effect in the Fe-Co bimetallic catalyst system for the growth of carbon nanotube forests. Journal of Applied Physics, 2015, 117, .	2.5	14
75	Interaction ofC60with Ge(111) in the33×33R30°phase: A(2×2)model. Physical Review B, 2000, 61, 1041	1 ଶ.0 416.	13
76	Thermal reactions at the interface between Si and C nanoparticles: nanotube self-assembling and transformation into SiC. Surface Science, 2003, 532-535, 886-891.	1.9	13
77	In situgrowth and thermal treatment of nanostructured carbon produced by supersonic cluster beam deposition: An electron spectroscopy investigation. Physical Review B, 2003, 67, .	3.2	13
78	Plasma stabilisation of metallic nanoparticles on silicon for the growth of carbon nanotubes. Journal of Applied Physics, 2012, 112, 034303.	2.5	13
79	Dynamics of the Si(100) surface. Surface Science, 1997, 377-379, 360-364.	1.9	12
80	Nitrile hydration to amide in water: Palladium-based nanoparticles vs molecular catalyst. Journal of Molecular Catalysis A, 2015, 410, 26-33.	4.8	12
81	Nanostructured TiOx film on Si substrate: room temperature formation of TiSix nanoclusters. Journal of Nanoparticle Research, 2010, 12, 2645-2653.	1.9	11
82	The photoinduced charge transfer mechanism in aligned and unaligned carbon nanotubes. Carbon, 2011, 49, 5246-5252.	10.3	11
83	Learning from Nature: Charge Transfer and Carbon Dioxide Activation at Single, Biomimetic Fe Sites in Tetrapyrroles on Graphene. Journal of Physical Chemistry C, 2019, 123, 3916-3922.	3.1	11
84	Mechanism of CO Intercalation through the Graphene/Ni(111) Interface and Effect of Doping. Journal of Physical Chemistry Letters, 2020, 11, 8887-8892.	4.6	11
85	Electronic structure and morphology of SiC films grown on Si(111) using C60 as a precursor. Surface Science, 2000, 454-456, 827-831.	1.9	10
86	Temperature-dependent interaction of C60 with Ge(1 1 1)-c(2 × 8). Applied Surface Science, 2003, 212-213, 52-56.	6.1	10
87	Atomic approach to core-level spectroscopy of delocalized systems: Case of ferromagnetic metallicMn5Ge3. Physical Review B, 2010, 81, .	3.2	10
88	Carbon nanotube forests growth using catalysts from atomic layer deposition. Journal of Applied Physics, 2014, 115, 144303.	2.5	10
89	TRACKING THERMALLY DRIVEN MOLECULAR REACTION AND FRAGMENTATION BY FAST PHOTOEMISSION: C60on Si(111). Surface Review and Letters, 2002, 09, 775-781.	1.1	9
90	Molecular orientation of C60 on Pt(111) determined by X-ray photoelectron diffraction. Applied Surface Science, 2003, 212-213, 57-61.	6.1	9

#	Article	IF	CITATIONS
91	Annealing Temperature Dependence of C60 on Silicon Surfaces Bond Evolution and Fragmentation as Detected by NEXAFS. Physica Scripta, 2005, , 695.	2.5	9
92	C KEdge NEXAFS of 6HSiC and 3CSiC Systems. Physica Scripta, 2005, , 308.	2.5	9
93	Effect of Oxygen Plasma Alumina Treatment on Growth of Carbon Nanotube Forests. Journal of Physical Chemistry C, 2014, 118, 18683-18692.	3.1	9
94	Surface states characterization in the strongly interacting graphene/Ni(111) system. New Journal of Physics, 2018, 20, 103039.	2.9	9
95	Carbon-based nanostructured materials via cluster beam deposition: a multi-technique investigation. Surface Science, 1998, 402-404, 441-444.	1.9	8
96	Photoemission of Ge(110) at room and high temperature. Surface Science, 1998, 402-404, 875-879.	1.9	8
97	Alignments of Carbon Nanotubes in Polymer Matrix: A Raman Perspective. International Journal of Polymer Analysis and Characterization, 2012, 17, 534-539.	1.9	8
98	Probing the electronic structure of multi-walled carbon nanotubes by transient optical transmittivity. Carbon, 2013, 57, 50-58.	10.3	8
99	Transport in polymer-supported chemically-doped CVD graphene. Journal of Materials Chemistry C, 2017, 5, 9886-9897.	5.5	8
100	Anomalous optical behavior in pyramid-like indium oxide (In2O3) nanostructures. Materials Science and Engineering B: Solid-State Materials for Advanced Technology, 2020, 262, 114781.	3.5	8
101	The electronic structure of the 3×3R30°–C60/Ge(111) system as measured by angle-resolved photoemission. Surface Science, 2000, 454-456, 514-518.	1.9	7
102	Sn on InSb(100)–c(2×8): growth morphology and electronic structure. Journal of Electron Spectroscopy and Related Phenomena, 2002, 127, 29-35.	1.7	7
103	Ferromagnetism in graphene-Mn(x)Si(1â^'x) heterostructures grown on 6H-SiC(0001). Journal of Applied Physics, 2012, 111, .	2.5	7
104	Carbon nanotube forests as top electrode in electroacoustic resonators. Applied Physics Letters, 2015, 107, .	3.3	7
105	Tuning graphene doping by carbon monoxide intercalation at the Ni(111) interface. Carbon, 2021, 176, 253-261.	10.3	7
106	Surface phase transitions of Ge(100) studied via valence band photoemission. Surface Science, 1998, 402-404, 871-874.	1.9	6
107	Tuning the charge state of a C60 single layer on Ag(1 0 0) by Na deposition. Surface Science, 2001, 482-485, 606-611.	1.9	6
108	Self-texturizing electronic properties of a 2-dimensional GdAu ₂ layer on Au(111): the role of out-of-plane atomic displacement. Nanoscale, 2017, 9, 17342-17348.	5.6	6

#	Article	IF	CITATIONS
109	The Effects of Cold Plasma Treatments on LDPE Wettability and Curing Kinetic of a Polyurethane Adhesive. Macromolecular Symposia, 2001, 169, 71-80.	0.7	5
110	Electronic properties of a pure and sodium-doped C70 single layer adsorbed on Al polycrystalline surface. Journal of Chemical Physics, 2005, 122, 054704.	3.0	5
111	Evidence for bandlike dispersion inK6C60(110)films. Physical Review B, 2006, 74, .	3.2	5
112	Micropatterned non-invasive dry electrodes for Brain-Computer Interface. , 2006, , .		5
113	Orientation ofC60molecules in the(33×33)R30°and(13×13)R14°phases ofC60â^•Ge(111)single layers. Phys Review B, 2008, 77, .	siçal 3.2	5
114	Tubular Sn-filled carbon nanostructures on ITO: Nanocomposite material for multiple applications. Carbon, 2013, 65, 13-19.	10.3	5
115	Quantum Confinement in Aligned Zigzag "Pseudoâ€Ribbons―Embedded in Graphene on Ni(100). Advanced Functional Materials, 2022, 32, 2105844.	14.9	5
116	SiC(111) growth by C60 decomposition on Si(111) studied by electron spectroscopies. Surface Science, 2001, 482-485, 829-835.	1.9	4
117	Metallic phases of a C70 single layer adsorbed on Cu(111) doped with sodium. Surface Science, 2003, 532-535, 892-897.	1.9	4
118	Oxidation of nanostructured Ti films produced by low energy cluster beam deposition: An X-ray Photoelectron Spectroscopy characterization. Thin Solid Films, 2012, 520, 4803-4807.	1.8	4
119	Viral Nanotemplates Armed with Oxygenic Polyoxometalates for Hydrogen Peroxide Detoxification. European Journal of Inorganic Chemistry, 2015, 2015, 3457-3461.	2.0	4
120	Conjugated polyelectrolyte nano field emission adlayers. Nanoscale Horizons, 2016, 1, 304-312.	8.0	4
121	Gold nanoparticles onto cerium oxycarbonate as highly efficient catalyst for aerobic allyl alcohol oxidation. Catalysis Communications, 2020, 140, 105989.	3.3	4
122	Electronic properties of carbon nanotubes as detected by photoemission and inverse photoemission. Nanotechnology, 2021, 32, 105703.	2.6	4
123	Ultra-high-vacuum epitaxial growth of MgB2(0001) thin films on Mg(0001) via molecular beam epitaxy. Journal of Physics Condensed Matter, 2004, 16, S3451-S3458.	1.8	3
124	Transient reflectivity on vertically aligned single-wall carbon nanotubes. Thin Solid Films, 2013, 543, 51-55.	1.8	3
125	Growth of hybrid carbon nanostructures on iron-decorated ZnO nanorods. Nanotechnology, 2016, 27, 145605.	2.6	3
126	Stable Fe nanomagnets encapsulated inside vertically-aligned carbon nanotubes. Physical Chemistry Chemical Physics, 2017, 19, 32079-32085.	2.8	3

#	ARTICLE	IF	CITATIONS
127	xmlns:mml="http://www.w3.org/1998/Math/MathML"> <mml:mrow><mml:msub><mml:mi>Ni</mml:mi><mml:m mathvariant="normal">C</mml:m </mml:msub></mml:mrow> electronic states in graphene-Ni(111) growth through resonant and dichroic angle-resolved photoemission at the C <mml:math xmlns:mml="http://www.w3.org/1998/Math/MathML"><mml:mi>K</mml:mi> -edge. Physical</mml:math 	n>23.2	11:mn>3
128	Review B, 2017, 96, . Can Atomic Buckling Control a Chemical Reaction? The Case of Dehydrogenation of Phthalocyanine Molecules on GdAu ₂ /Au(111). Journal of Physical Chemistry C, 2019, 123, 6496-6501.	3.1	3
129	Ultrathin Fullerene-Based Films via STM and STS. , 2008, , 1-21.		3
130	Thermally induced changes in cluster-assembled carbon nanocluster films observed via photoelectron spectroscopy. Applied Surface Science, 2003, 212-213, 879-884.	6.1	2
131	Cepeket al.Reply. Physical Review Letters, 2004, 93, .	7.8	2
132	Graphene islands mixed to carbon nanostructures grown on TiN film: A multiâ€ŧechniques characterization approach. Physica Status Solidi (B): Basic Research, 2012, 249, 2519-2521.	1.5	2
133	Organic Molecules on Noble Metal Surfaces: The Role of the Interface. , 0, , .		2
134	Defect states in ZnO/SnO2 composite nanostructures (CNs) for possible facilitating role in carrier transport across the junction. Journal of Materials Science: Materials in Electronics, 2021, 32, 1818-1828.	2.2	2
135	Fast-tracking of NH3 interaction with ZnO nanorods and C/ZnO hybrid nanostructures by operando spectroscopy. Applied Surface Science, 2022, 590, 153067.	6.1	2
136	ULTRA THIN C ₆₀ -BASED FILMS: MOLECULAR ARRANGEMENT AND ELECTRONIC STATES. , 2001, , .		0
137	Influence of impurities on the density of states at the fermi level in the c(6×4)-C60/Ag() two-dimensional superstructure. Nuclear Instruments & Methods in Physics Research B, 2003, 200, 1-4.	1.4	0
138	Band-like dispersion in the valence band photoemission spectra of K6C60(110) films. AIP Conference Proceedings, 2005, , .	0.4	0
139	Suppressed Hysteretic Field Emission from Polymer Encapsulated Silver Nanowires. IEEE Nanotechnology Magazine, 2016, , 1-1.	2.0	0
140	C60 monolayer on semiconductors. , 2018, , 769-774.		0
141	Ordered fullerenes on metal surfaces: monatomic steps on vicinal surfaces and reconstruction on metals. , 2018, , 764-768.		0
142	Co-adsorbed fullerene systems and the formation of heterojunction layers at a nanometer scale. , 2018, , 784-788.		0